A Theoretical Study of the Formation of the Aminoacetonitrile Precursor of Glycine on Icy Grain Mantles in the Interstellar Medium

Denise M. Koch,[†] Céline Toubin,[‡] Gilles H. Peslherbe,[§] and James T. Hynes*,[†,£]

Département de Chimie, Ecole Normale Supérieure, UMR 8640 PASTEUR, 24 rue Lhomond, Paris, F-75005 France, Laboratoire de Physique des Lasers, des Atomes et des Molécules, Université de Lille I, Cité Scientifique, 59655 Villeneuve d'Ascq Cedex, France, Centre for Research in Molecular Modeling and Department of Chemistry & Biochemistry, Concordia University, 7141 Sherbrooke Street West, Montreal, Quebec H4B 1R6, Canada, and Department of Chemistry and Biochemistry, University of Colorado, Boulder, Colorado 80309-0215

Electronic structure calculations have been carried out for one of the key reactions in a Strecker synthesis route to the amino acid glycine, in connection with amino acid production in the interstellar medium (ISM). Density functional calculations at the B3LYP/6-31+G(d,p) level have been performed for the reaction between methanimine, CH_2NH, and the two isomers HNC/HCN, leading to aminoacetonitrile—a known precursor of glycine—in both the gas phase and on a model icy grain surface. Three mechanisms are evidenced in the reference gas-phase calculations; for CH_2NH reacting with HCN, there are two routes referred to as indirect and direct, and for CH_2NH reacting with the isomer HNC, a one-step mechanism is found. All of these reaction paths have quite high barriers, but on a model interstellar grain icy surface, very considerable barrier reduction results due to a concerted proton relay mechanism. Explicit water molecules in a reaction ring are shown to participate in this relay mechanism in the reactions of CH_2NH both with HCN and with the HNC isomer. The inclusion of two explicit H_2O molecules leads to the strongest effect for the concerted proton transfer. With several further solvating waters included, this proton relay route to aminoacetonitrile for the HNC isomer via a direct mechanism is found to have a very low free-energy barrier at 50 K, $\Delta G_{50K} < 1$ kcal/mol, and thus appears to be feasible in the ISM. The corresponding reaction with HCN, however, has a much higher barrier, $\Delta G_{50K} = 7$ kcal/mol. The significance of these results for glycine production in the ISM is discussed.

I. Introduction

The origin of amino acids in the prebiotic chemistry of the early Earth has been a topic of long-standing interest.[1] In one view,[2,3] amino acids may have originated in the interstellar medium (ISM) and were then transported to earth, a scenario supported by the finding of amino acids in meteorites[4] and following UV irradiation of interstellar ice models.[2] While the detection of glycine, the simplest amino acid, in the ISM is controversial,[5] the possibility of its existence in the ISM encourages the investigation of the molecular mechanisms of the production of amino acids in the ISM. In this paper, a theoretical study of the formation of an important precursor of glycine, aminoacetonitrile, on a model amorphous[6] ice surface is presented.

Among the possible ways to produce amino acids and their precursors, special attention has been given to the possibility of a prebiotic Strecker synthesis starting from formaldehyde and ammonia[7] (Scheme 1) in the ISM at the surface of interstellar ice ("icy grain") particles.[8,9]

The focus of the present work is on the production of aminoacetonitrile, H_2NCH_2CN, whose formation is the penul-

SCHEME 1
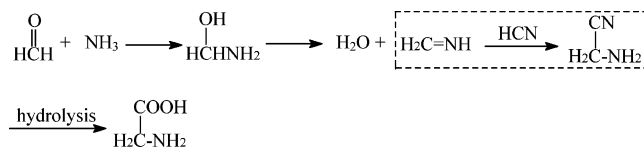
timate step, prior to hydrolysis of aminoacetonitrile to form glycine, and which is believed to be the central crossroads of the Strecker synthesis system.[10,11] This step involves the addition of hydrogen cyanide (HCN) to methanimine (CH_2NH), both of which are long-lived molecules in the ISM; see the outlined portion in Scheme 1.[8,9,12] In a previous theoretical study, Arnaud et al. considered a three-step mechanism for the formation of aminoacetonitrile from HCN and methanimine and found significant gas-phase reaction barriers for the stepwise process.[10] (A similar study of this gas-phase mechanism was carried out by Basiuk via DFT calculations, with similar conclusions.[13]) Consideration by Arnaud et al. of solvation by an aqueous medium through a polarizable dielectric continuum model reduced the barrier by about 25 kcal/mol for the rate-determining step due to solvation of zwitterionic transition structures.[10] However, this lowering was shown to be insufficient to render the reaction feasible under ISM conditions.[8,9,12]

In this paper, the formation of aminoacetonitrile via the addition reaction of methanimine and HCN (boxed section of Scheme 1) is reconsidered by means of density functional

---
* To whom correspondence should be addressed. E-mail: hynes@chimie.ens.fr.
  † Ecole Normale Supérieure.
  ‡ Université de Lille I.
  § Concordia University.
  £ University of Colorado

Formation of the Aminoacetonitrile Precursor of Glycine

J. Phys. Chem. C, Vol. 112, No. 8, 2008 **2973**

electronic structure calculations, with the inclusion of the possibility that the reaction occurs with the HNC isomer. HNC is a well-known constituent of cold molecular clouds and is ubiquitous in comets.[14] In cold interstellar clouds, HNC has an abundance which can approach or even exceed that of HCN. Both HCN and HNC presumably also exist in the icy dust grain mantles due to sticking at the surface, although neither has actually been detected in icy grains.[14]

We find that the reaction between HNC and methanimine to produce aminoacetonitrile is found to proceed via a route not previously considered, namely, a proton relay mechanism involving several water molecules. Interestingly, proton relay mechanisms have previously been found theoretically in heterogeneous reactions on ice in connection with stratospheric ozone depletion[15] and for an initial step in the Strecker synthesis.[16] The calculated barrier height for the HNC reaction (although not for the HCN reaction) is sufficiently low for the reaction to be viable in the ISM.

The outline of the remainder of the present paper is as follows. After a description of the computational methods in section II, the detailed gas-phase mechanisms to form aminoacetonitrile via HCN or HNC reaction with CH_2CN are presented in section III. Section IV describes the results of adding explicit water molecules in a reaction ring to allow a proton relay process. The consequences of additional explicit solvation are discussed in section V, and section VI concludes.

II. Computational Details

All of the calculations within have been performed using the GAMESS program.[17] Arnaud et al.[10] have demonstrated the reliability of calculations performed with the Becke three parameter hybrid functional and the correlation functional of Lee, Yang, and Parr (B3LYP).[18] Their calculations indicate that the geometries predicted by the B3LYP/6-31+G(d,p) model chemistry are similar to those obtained with second-order Møller−Plesset (MP2) theory, and the energetics of the reactions are in relatively good agreement with those calculated with the very reliable G2(MP2) procedure. Further, a previous study by Basiuk[19] has shown that the 6-31+G(d,p) basis set[20] associated with the B3LYP hybrid density functional model gives reliable results for the investigation of such reactions, on the basis of calculations comparing a large number of basis sets. Consequently, all of the present computations were carried out with B3LYP using the 6-31+G(d,p) basis set. The stationary point geometries were fully optimized and characterized as minima (no imaginary frequencies) and first-order saddle points (one imaginary frequency), transition states, by normal-mode analysis.[21] All the optimizations met a convergence criteria of 10^{-7}. The search for transition states was carried out by using the gradient extremal method[22] with the Sun and Ruedenberg algorithm.[23] The connection between the different transition states and reaction intermediates was ensured by intrinsic reaction coordinate (IRC) calculations with step sizes of 6 and 10 (in units of 0.01 amu$^{-1/2}$ Bohr). Zero point energies (ZPEs) were obtained from harmonic vibrational frequency calculations. In order to account for the low temperatures (a few tens of Kelvin) of the ISM,[8,12] thermochemical data were calculated at 50 K, again employing harmonic vibration frequencies.

III. The Gas-phase Pathways for HCN + CH_2NH and HNC + CH_2NH: Energetics and Continuum Solvation

In this section, we present and discuss, as an important preliminary for subsequent sections, the results for the mechanisms of the separate reactions of CH_2NH with HCN and HNC,
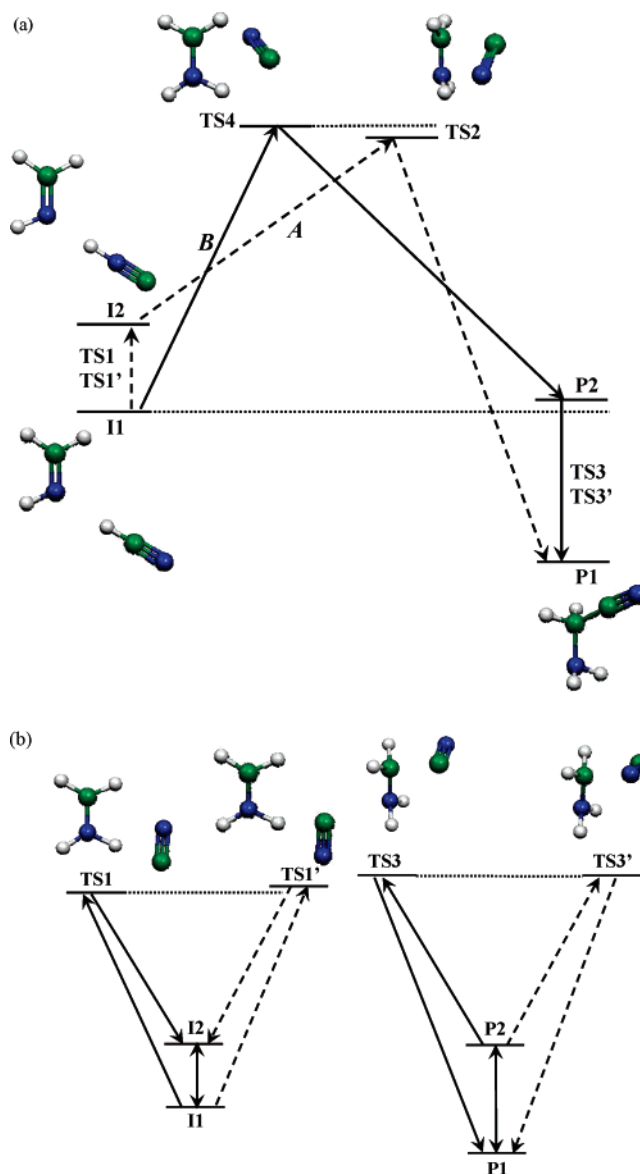
Figure 1. (a) Indirect path *A* (dashed line) and direct path *B* (solid line) for the gas-phase reaction CH_2NH + HCN → CH_2NH_2CN. The color scheme for the atoms is blue for N, green for C, and white for H. For their optimized structures, see Figure 3. (b) Details of the two isomerization mechanisms through routes *A* and *B*.

without any waters involved and calculated using the computational methods described in section II. Solvent free energetic effects on these "gas-phase" reactions are then assessed by a simple continuum dielectric model.

IIIa. Overall Pathways and Energetics. The essentials of the calculated gas-phase pathways are summarized in Figure 1a. The reaction with HCN is first discussed and starts with the HCN complexed to the imine, here labeled **I1**, with the "I" nomenclature indicating an intermediate on the reaction pathway with respect to the separated HCN and methanimine. There are two reaction pathways, labeled *A* and *B*, leading to aminoacetonitrile. Pathway *B* involves the direct addition of HCN to methanimine going through a transition state **TS4** to an intermediate product labeled **P2**, which is the isomer H_2-NCH_2NC of aminoacetonitrile (H_2NCH_2CN). A subsequent isomerization step converts **P2** to the aminoacetonitrile product H_2NCH_2CN (**P1**), passing through two possible transition states **TS3** or **TS3′**, which are discussed in more detail below. This entire pathway *B* is referred to as the "direct" mechanism for
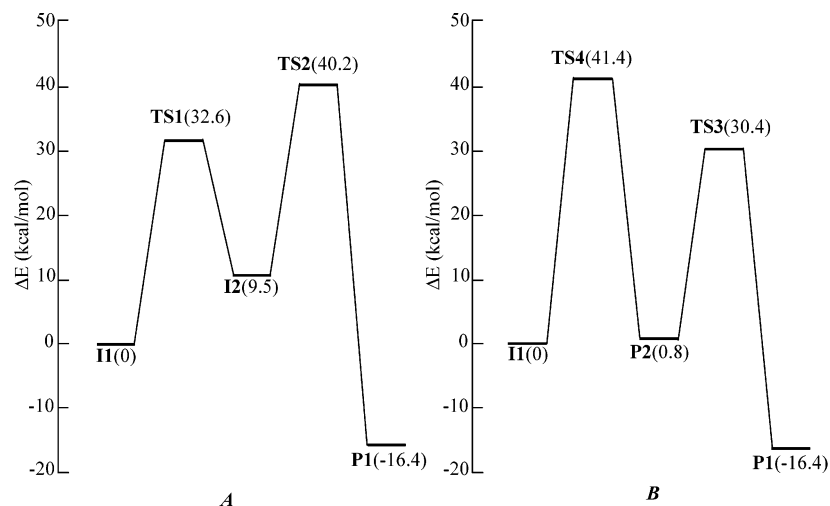
Figure 2. Relative energy profile (in kcal/mol, ZPE-corrected values) along the indirect *A* and direct *B* pathways shown in Figure 1 for the gas-phase CH_2CN + HCN. For optimized structures of the intermediates, see Figure 3.

TABLE 1: Comparison of the 0 K Relative Energies (in kcal/mol) from the Present Work with Previous Calculations

	this work[a]	B3LYP[b,c]	HF[b,c]	MP2[b,c]	QCISD(T)[b,c]	G2MP2[b]	B3LYP[d]
I1	0	0	0	0	0	0	0
TS1	32.6	32.5	32.3	34.3	34.2	32.2	
TS1′	33.4						33.5
I2	9.5	9.7	7.2	14.0	11.5	10.9	
TS2	40.2	39.0	34.9	42.7	42.2	41.2	40.3
TS4	41.4						
P1	−16.4	−19.7	−19.0	−19.9	−16.2	−16.5	−17.1
TS3	30.4						31.2
TS3′	30.4	28.8		34.2	34.1	33.3	
P2	0.8	−2.4	−5.2	0.9	0.5	1.5	

[a] Calculated with B3LYP/6-31+G(d,p). [b] From Table 1 of ref 9. [c] Using a 6-31+G(d,p) basis set. [d] From Figure 1 of ref 12.

reaction with HCN, to be distinguished from the "indirect" mechanism *A*. Pathway *A* involves the isomerization of HCN to HNC from the initial complex **I1** to produce **I2**, proceeding through two possible transition states **TS1** or **TS1′**. The isomerized intermediate **I2** then proceeds through a transition state **TS2** to reach the desired aminoacetonitrile product (**P1**). Notice that both the direct *B* and indirect *A* pathways out of the HCN−imine complex (**I1**) involve two steps; for *B*, one has a C−N≡C bond formation step followed by an isomerization to produce the C−C≡N bond, while for *A*, a HCN → HNC isomerization occurs first in the complex with the imine, followed by the C−C≡N bond formation step. It will prove very important for later considerations that the reaction from the isomerized complex **I2**, that is, involving the HNC isomer rather than HCN, produces aminoacetonitrile (**P1**) in a single step.
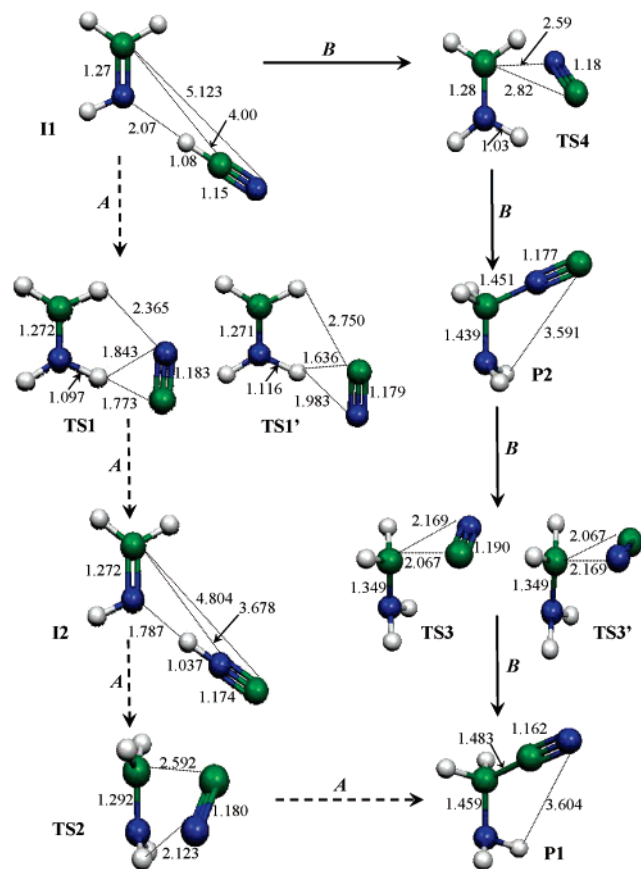
We pause to return to the relatively minor issue of the pairs of transition states for the isomerization steps for pathway *A*, **I1** to **I2**, and pathway *B*, **P1** to **P2**. As Figure 1b illustrates, the CN group can rotate in either of two directions within the complex, resulting in two transition states for each isomerization reaction. The **I1**/**I2** isomerization transition states **TS1** and **TS1′** differ slightly in energy (0.8 kcal/mol), reflecting an asymmetry due to the differing neighbor atoms. For the **P1**/**P2** isomerization, the environment is more symmetric, and the transition states **TS3** and **TS3′** are isoenergetic.

Figure 2 gives the calculated zero temperature energy profiles for the two reaction pathways *A* and *B* of Figure 1, with the one-step pathway from the methanimine−HNC complex **I2** included as the sequence **I2** → **TS2** → **P1**. Starting from the **I1** complex, the barriers for both pathways are very high, between 30 and 40 kcal/mol, and starting from the **I2** complex, a high

barrier of ∼30 kcal/mol must be surmounted. The 0 K energetics obtained in this work are compared to those obtained by Arnaud et al.[10] and Basiuk[13] in Table 1, and they are generally in good agreement with the DFT calculations performed in those previous studies. However, the energies of **I2**, **P2**, and some of the transition states are, in general, lower in energy than those obtained with higher-level model chemistries [MP2, QCISD-(T)] and the G2(MP2) method.[24]

IIIb. Transition-State Structures. There are both similarities and differences of the present results with those in previous work. Figure 3 presents the optimized geometries of the stationary and transition species for the gas-phase reactions of CH_2NH + HCN and CH_2NH + HNC using B3LYP/6-31+G-(d,p). The **I1**, **I2**, **P1**, **P2**, and **TS2** structures are the same as those reported by Arnaud et al.[8] Further, the transition states **TS1** and **TS3′** obtained in this work have the same structures as the transition states referred to as "TS1" and "TS3" by Arnaud et al.[10] However, transition states **TS1′**, **TS3**, and **TS4** were not reported by these authors. Interestingly, the **TS1′** and **TS3** transition states obtained herein are very similar to those termed by Basiuk as "TS1" and "TS3", although the geometrical parameters are slightly different, probably due to the larger basis set [6-311++G(d,p)] used in that work.[13] The structures **TS1**, **TS3′**, **TS4**, **I2**, and **P2** are not mentioned in ref 12. In summary, the authors of refs 9 and 12 did not consider both orientations of the CN moiety for the isomerization steps (**I1** → **I2** and **P1** → **P2**) and did not consider the pathway from **I1** to **P2** via **TS4**.

IIIc. Free-Energy Changes and Continuum Solvation Issues. Arnaud et al. also presented 298 K gas-phase reaction free energies together with the 298 K free-energy results including equilibrium, dielectric continuum, and solvation

Formation of the Aminoacetonitrile Precursor of Glycine

J. Phys. Chem. C, Vol. 112, No. 8, 2008 **2975**

Figure 3. Optimized geometries calculated at the B3LYP/6-31+G-(d,p) level of theory for the intermediates and transition states situated along the indirect *A* and direct *B* pathways. The color scheme for the atoms is blue for N, green for C, and white for H. Interatomic distances are given in Å.

treated via the polarizable continuum model (PCM).[25] The gas-phase 298 K free-energy ΔG values (ZPE included) calculated in the present work agree to within 1/2 kcal/mol for those stationary and transition-state points which are in common with ref 9. The remaining G values, with **I1** taken as the zero of free energy, are, in kcal/mol, **TS1′**, 32.6; **TS3**, 30.4; **TS4**, 41.4. The 298 K free energies G_s using the standard PCM model included in the GAMESS program were calculated at the gas-phase geometries.[17] The present results share with those of ref 9 the conclusion that certain barriers are reduced by solvation due to largely separated net charges in the transition states. The net Mulliken charges,[26] that is, the sum of the atomic charges, for atoms N and C of HNCH$_2$ and H, C, and N of HCN or HNC are -0.563 for **I1** (ΔG(PCM) = 0.0 kcal/mol, selected as the reference), -0.590 for **I2** (ΔG(PCM) = -3.0 kcal/mol), -0.861 for **TS1** (ΔG(PCM) = -23.0 kcal/mol), -0.75 for **TS2** (ΔG(PCM) = -11.1 kcal/mol), -0.781 for **TS3** (ΔG(PCM) = -19.8 kcal/mol), -0.829 for **TS4** (ΔG(PCM) = -21.1 kcal/mol), -0.677 for **P1** (ΔG(PCM) = -6.5 kcal/mol), and -0.643 for **P2** (ΔG(PCM) = -8.4 kcal/mol). The best solvation occurs for **TS1** and **TS4**, then **TS2** and **TS3**, and finally **P1** and **P2**, which is consistent with the ordering of their net Mulliken charges. However, there are numerical differences concerning the dielectric continuum free energetics; for example, **TS1** and **TS4** lie 20.6 and 14.1 kcal/mol, respectively, above **I1** in the present calculations, whereas ref 9 gives 13.0 and 9.9 kcal/mol. These differences,[27] while non-negligible, only reinforce the conclusion evident from ref 9 that dielectric continuum solvation will not render the production of aminoacetonitrile feasible under

the low-temperature conditions of the ISM. Different considerations are required, taken up in the next section.

## IV. Evidence for a Concerted Proton Relay Mechanism

IVa. Proton Relay Mechanism. As discussed above, even with dielectric continuum solvation, the free-energy barriers for the production of aminoacetonitrile from methanimine and hydrogen cyanide isomers remain too large for the reaction to be feasible under low-temperature ISM conditions. In this section, a "catalytic" alternative for the heterogeneous reaction on icy grain surfaces is considered.

Attention to the chemistry involved in the reaction provides an indication of an alternative pathway. Focusing first on transition state **TS4** in Figure 1, the nucleophilic attack of the nitrogen of the HCN moiety to form the new CN bond is accompanied by the transfer of a proton from the HCN unit to the N of the imine to form a NH bond. An analogous scenario characterizes transition state **TS2** in Figure 1a, that is, the attack of C on the imine carbon to form a new CC bond is accompanied by a proton transfer from the HNC moiety to the N of the imine to form a NH bond. Catalytic coupled nucleophilic attack/proton transfer via a chain of water molecules has already been found theoretically for heterogeneous reactions on ice of importance in stratospheric chemistry.[15,16,28] Thus, a "catalytic" proton relay mechanism via explicit inclusion of water molecules in a ring structure with the reactants is now explored.

It will later be shown that two explicit water molecules in the ring prove to be optimal, and we focus on that case here. Upon consideration of the methanimine/HCN complex **I1** in Figure 1a as the starting point, an issue arises as to where to place two H$_2$O molecules with respect to HCN and CH$_2$CN for an efficient reaction. From the point of view of an analogue of pathway *B* in Figure 1a, that is, a required attack of the HCN nitrogen on the C of the imine, the **I1**·2H$_2$O configuration shown in Figure 4a is an obvious candidate. As schematically shown in this figure, on the one hand, the attack to form the desired CN bond is geometrically favored, while on the other hand, a proton could transfer from HCN through the two water molecule chain, ultimately to form a NH bond with the former imine. The schematic Figure 4b illustrates how an analogous initial complex **I2**·2H$_2$O involving the HNC isomer could allow a proton relay chain involving CC formation. This initial **I2**·2H$_2$O complex would be the natural product of the HCN/HNC isomerization from the **I1**·2H$_2$O complex in Figure 4a, that is, the proton relay version of the first, isomerization, step in pathway *A* in Figure 1.

The optimized **I1**·2H$_2$O structure is shown in Figure 4a. For completeness, two other complexes of **I1** with two water molecules were also calculated. The first is the structure called "Ia" in ref 9, in which the HCN is placed between two water molecules, the latter completing a ring with the methanimine, and the second is a structure where the HCN is complexed to the N of the imine, the two water molecules then completing the chain with a methylene H. The **I1**·2H$_2$O complex, shown in Figure 4a, is the most stable of the three, by 2.4 and 2.9 kcal/mol, respectively. No further complexes with the two H$_2$O molecules were considered since the **I1**·2H$_2$O structure appeared to be an ideal configuration for both the reaction scheme and the complex stability. In the language of ref 12, the two water molecule complex in Figure 4 is hereafter referred to as the core reaction system (CRS).
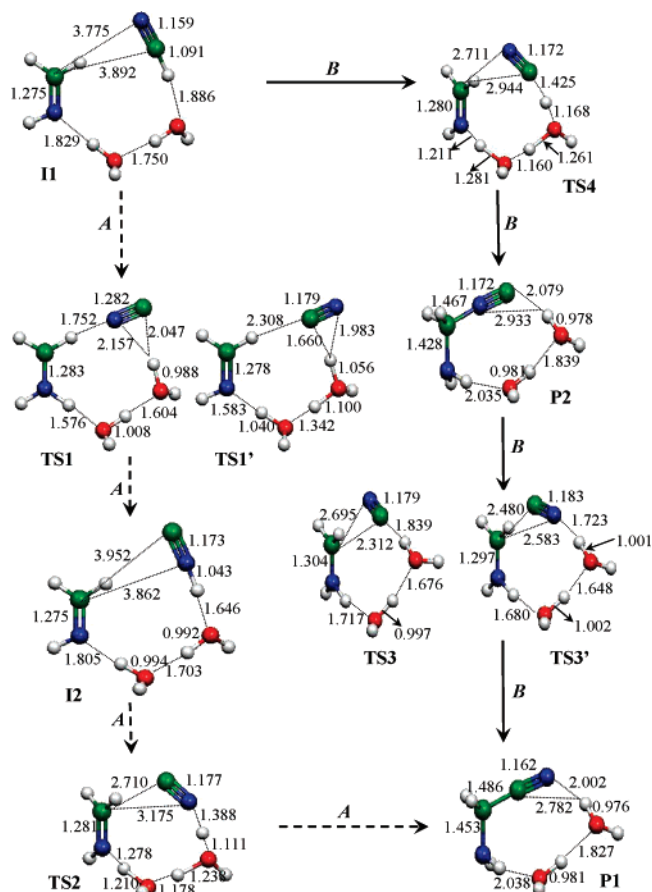
IVb. Structures and Energetics of the Two Water Core Reaction Systems. We now discuss the calculations and results

(a) **I1·2H₂O**

(b) **I2·2H₂O**
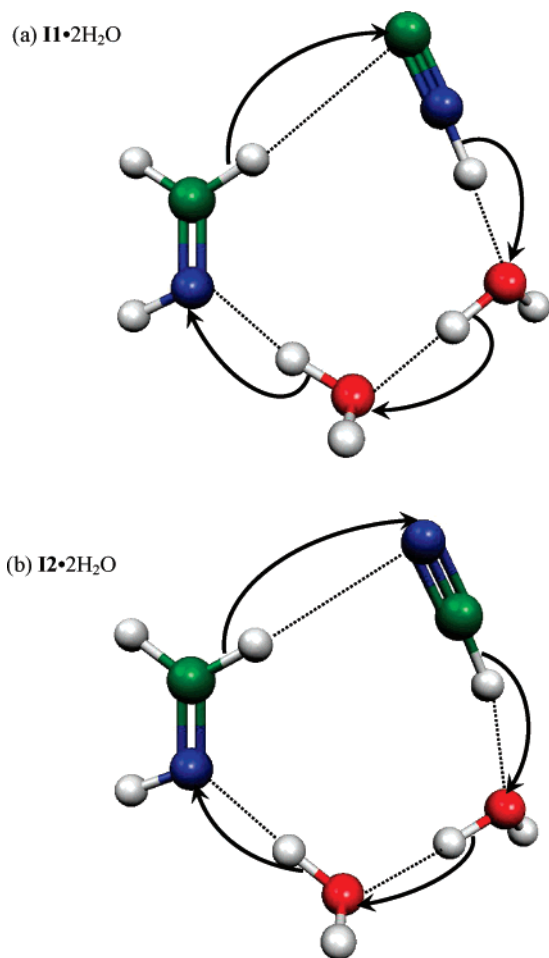
Figure 4. Schematic representation of the complex of methanimine with (a) HCN and (b) HNC and two water molecules within a proton relay ring.


Figure 5. Optimized geometries at the B3LYP/6-31+G(d,p) level of theory of the intermediates situated along the indirect *A* and direct *B* pathways starting from the core reaction system = $CH_2NH + HCN + 2 H_2O$ in the ring. The color scheme for the atoms is blue for N, green for C, red for O, and white for H. Interatomic distances are given in Å.

of the pathways for aminoacetonitrile production in terms of the core reaction system (CRS) (Figure 4). The computational challenges posed by the larger CRS compared to the gas phase has forced us to adopt a somewhat altered procedure compared to that case. In particular, the CRS is too large to perform IRC calculations. Since the ring water molecules in the CRS play essentially a proton-transfer role, facilitating the basic transformations of the gas-phase pathways, the reaction starting with the **I1·2H₂O** complex is assumed to follow a globally similar pathway. The transition states for the CRS system are obtained by the gradient extremal method described in section II and are confirmed by obtaining first-order saddle points (one imaginary frequency) from normal-mode analysis (rather than by an IRC analysis). This basic approach is supported by the finding, discussed below, that, for example, the CC and CN distances in the nucleophilic attack transition states are not significantly different from the values found in the gas-phase reaction.

Figure 5, with the associated energetic diagram shown in Figure 6, details the mechanisms found for the CRS along the analogues of the gas-phase pathways *A* and *B*. Indeed, the *A* and *B* pathway notation is retained in all that follows. In the left column of Figure 5, the indirect mechanism for the HCN/methanimine complex **I1·2H₂O** commences with the **I1·2H₂O** isomerization to **I2·2H₂O** involving the HNC isomer, via **TS1· 2H₂O** or **TS1′·2H₂O**. The nucleophilic attack then proceeds through **TS2·2H₂O**, generating a new CC bond and ultimately reaching **P1·2H₂O**, the complex of aminoacetonitrile and 2 H₂O.

On the right-hand side of Figure 5, the direct mechanism *B* involving HCN, with **I1·2H₂O** as an initial reactant, proceeds through the nucleophilic attack transition state **TS4·2H₂O**, with a new CN bond formed to produce **P2·2H₂O**. Then, **P2·2H₂O** isomerizes through either the **TS3′·2H₂O** or **TS3′·2H₂O** transition state to generate the desired CC bond in the aminoacetonitrile complex **P1·2H₂O**.

As noted below, on the structural view of Figure 5, the configurations of the transition states for the two water CRS reactions are similar to the gas-phase ones obtained and displayed in Figure 3. For example, the distances between C of CH₂NH and N of NCH or C of CNH are comparable (CRS values listed first, gas-phase values second): **TS4**, 2.711 Å, 2.596 Å; **TS2**, 2.710 Å, 2.592 Å; **TS3**, 2.695 Å, 2.169 Å; **TS3′**, 2.480 Å, 2.067 Å.

Figure 6 shows the considerable barrier reduction for the proton relay mechanism compared to the gas-phase values and is further detailed in Table 2. The presence of catalytic water molecules greatly reduces the conformational changes between the reaction species relative to the gas phase and facilitates the transfer of a proton from the cyanide moiety to the nitrogen atom on methanimine, therefore significantly reducing the reaction barriers for all pathways. We return to this point at the conclusion of this section.

IVc. Variation of the Number of Waters in the Ring. In the CRS system just discussed, we have explored two H₂O's in the ring scheme. Here, we briefly present results indicating that, as anticipated at the beginning of this section, this is an optimum

Formation of the Aminoacetonitrile Precursor of Glycine

J. Phys. Chem. C, Vol. 112, No. 8, 2008 **2977**
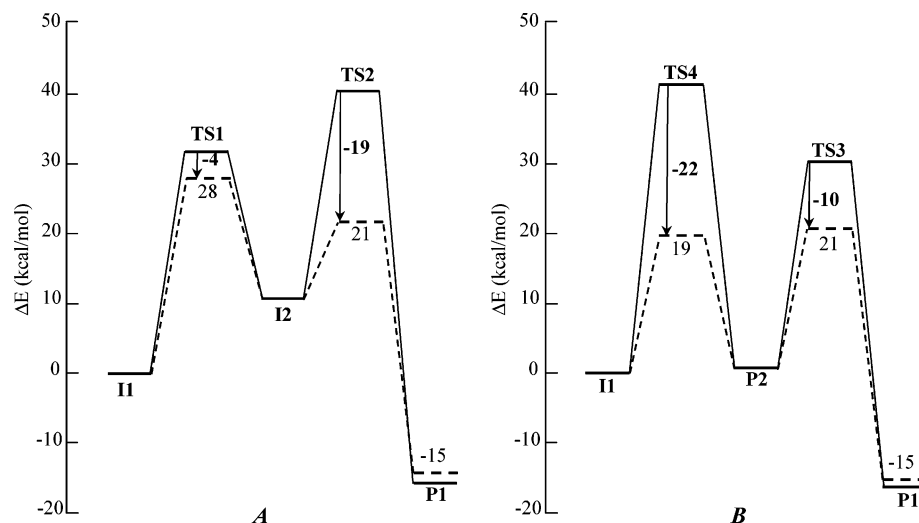
Figure 6. Relative ZPE-corrected energy profile (kcal/mol) calculated at B3LYP/6-31+G(d,p) along both the indirect *A* and direct *B* pathways for the reaction CH_2NH + HCN in the gas phase (solid line) and with two H_2O's in the core reaction system (dash line). The stabilization induced by the two H_2O molecules is also given in kcal/mol on the right-hand side of a vertical arrow. For optimized structures of the intermediates, see Figure 5.

TABLE 2: Relative Thermodynamic Contributions (in kcal/mol) Calculated at 298 K and at 50 K; For the Reaction $HNCH_2 \cdot nH_2O + HCN \rightarrow NH_2CH_2CN \cdot nH_2O$ in the Gas Phase, $n = 0$, and with nH_2O, $n = 1, 2, 3$, in the Core Reaction System[a]

	I1	TS1	TS1′	I2	TS2	TS4	P1	TS3	TS3′	P2
					$n = 0$					
ΔE	0	32.6	33.4	9.5	40.2	41.4	−16.4	30.4	30.4	0.8
ΔG_{298K}	0	33.9	34.5	9.9	41.7	42.7	−14.2	32.3	32.3	2.9
ΔG_{50K}	0	32.1	33.0	9.4	39.8	41.0	−16.9	30.0	30.0	0.3
					$n = 1$					
ΔE	0	30.0	31.8	9.6	26.4	25.6	−14.2	25.4	25.3	3.5
ΔG_{298K}	0	33.3	35.0	10.9	29.9	29.2	−11.4	28.9	28.8	5.9
ΔG_{50K}	0	29.5	31.3	9.3	25.8	25.0	−14.4	25.0	24.9	3.4
					$n = 2$					
ΔE	0	28.2	32.6	9.2	21.1	19.4	−15.3	20.9	20.6	2.5
ΔG_{298K}	0	30.4	34.9	9.5	24.5	22.8	−13.0	23.7	23.8	4.8
ΔG_{50K}	0	27.6	31.8	9.1	20.3	18.6	−15.7	20.3	20.1	2.1
					$n = 3$					
ΔE	0		33.1	9.2	22.9	20.5	−14.1	20.3	20.0	4.7
ΔG_{298K}	0		35.7	9.6	26.6	24.2	−11.6	23.1	23.1	7.1
ΔG_{50K}	0		32.4	9.2	21.9	19.5	−14.5	19.6	19.4	4.4

[a] Calculated with B3LYP/6-31+G(d,p). For optimized structures, refer to Figures 3 and 4.

choice. The results with nH_2O's, $n = 0-3$, included in the ring (see Table 2) are summarized in Figure 7. The energy of transition state **TS4** located along the pathway *B* in Figure 5 is referenced to that of the reaction complex $I1 \cdot nH_2O$, while that of transition state **TS2** located along pathway *A* is referenced to both the $I1 \cdot nH_2O$ and $I2 \cdot nH_2O$ complexes. It is seen that the incorporation of one to two water molecules into the ring stabilizes both transition states, with two H_2O's being optimal for reducing the barrier heights since the addition of a third H_2O tends to increase the barriers. Table 2 details the energetics and free energetics and shows that the choice of $n = 2$ for the number of waters in the ring is optimal in terms of free-energy barriers at the low temperature of 50 K representative of the ISM.

In summary, it has been shown in this section that catalytic proton transfer is optimal when two waters form a ring with
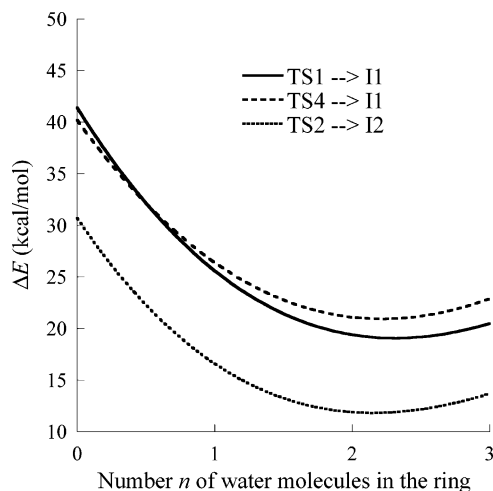
Figure 7. Variations of the transition states' relative energies (ZPE-corrected) calculated at the B3LYP/6-31+G(d,p) level as a function of the number n of water molecules included in the core reaction system.

the reactants and that this transfer lowers the free-energy barriers considerably in comparison to those in the gas phase. Nonetheless, these barriers remain important. For example, the 50 K free-energy barrier for **TS2** starting with the HNC isomer/imine complex with two waters ($I2 \cdot 2H_2O$) is still ∼20 kcal/mol. This suggests that attention is required to external solvation, as now discussed.

## V. External Solvation by Additional Waters

Since catalysis of the reaction via a proton relay bridge does not itself suffice to reduce the reaction barriers sufficiently for the reaction to occur under the low-temperature conditions in the ISM, the solvation of the core reaction systems by the addition of explicit water molecules around the various reaction species is now explored. An immediate issue arises as to where the solvating water molecules should be initially positioned around the CRS reaction ring (prior to geometry optimizations). Some key characteristics of the CRS reaction paths have been considered to help assign these positions: (i) the important partial charges present in the CRS, focusing especially on transition states and (ii) the proton-transfer bridge, with its shifting positive charge. The positions of the solvating water

molecules were chosen so as to stabilize the atoms with significant partial charges, corresponding to the dangling hydrogen atoms of the water molecules within the CRS, the C and N of HCN/HNC, and the N of the imine, involving five water molecules. However, initial calculations showed that the addition of only five external waters was insufficient, for the following reason. The positions of these five external solvating waters were found to shift significantly (between 1 and 4 Å) along the reaction pathways due to conformational changes in the CRS, a phenomenon which would not be expected from water molecules frozen in the amorphous ice lattice of an icy grain mantle. In order to eliminate this nonphysical behavior, the positions of 12 external solvating waters were chosen via the procedure now described. The structures of all of the CRS reaction species with the optimized positions of the five solvating water molecules were superimposed, where the CN bond of the methanimine species served as a reference to superimpose the solvated CRS structures (see Figure 5). For each reaction pathway, this procedure resulted in 5 superimposed structures and therefore 25 water molecules around the super-imposed core reaction systems. This procedure generated a number of solvating water molecules in these superimposed structures which had very similar positions, that is, waters that were on top of each other with less than 0.5 Å difference in their oxygen atom locations, an obvious physical impossibility due to repulsive forces. Accordingly, all but one of these waters were removed, such that 12 external solvating water molecules were retained for each reaction species. The positions of the external solvating waters were then optimized for each reaction species, while keeping the positions of the CRS atoms and the oxygen atoms of the external solvating waters fixed. None of the hydrogen atoms for these 12 remaining waters moved more than 0.2 Å in the various reaction pathways, thus providing the desired mimic of the icy grain mantle surface environment.

The geometries of the CRS·12H$_2$O system for pathway *A* are shown in Figure 8. Since the complete CRS·12H$_2$O system is difficult to visualize, only the water molecules directly hydrogen-bonded to the CRS are shown in Figure 8. The solvating waters, which directly stabilize the CRS atoms with large partial charges, for each reaction species are connected to the CRS by dotted lines. The remaining solvating water molecules mimic an amorphous ice lattice.

The relative thermodynamic contributions for the CRS·12H$_2$O system are summarized in Table 3. $\Delta G^{\ddagger}_{50K}$ and $\Delta E^{\ddagger}$ are relative values with respect to the corresponding stable intermediates: **I1** as a reference for **TS1** and **TS4**; **I2** as a reference for **TS2**; and **P2** as a reference for **TS3**. $\Delta\Delta G^{\ddagger}_{50K}$ and $\Delta\Delta E^{\ddagger}$ quantify the effect of the external solvent contribution on the CRS thermodynamics and, especially, the net transition-state stabilization that arises due to external solvation. As can be seen from Table 3, the explicit external solvation of the CRS lowers the reaction barriers by between 10 and 20 kcal/mol.

Figure 9 presents the 50 K free-energy profile of the CRS· 12H$_2$O for pathways *A* and *B*. Recall that mechanism *A* corresponds to an indirect pathway from HCN and a one-step path from HNC, while mechanism *B* corresponds to a direct pathway from HCN (Figure 1). For the key one-step mechanism with HNC as a reactant, that is, starting with **I2** in mechanism *A*, the free-energy barrier is only 0.7 kcal/mol at 50 K; in addition, this reaction is favored over the back reaction of HNC/ HCN isomerization to re-form complex **I1**, whose free-energy barrier of 1.5 kcal/mol is higher. Starting from HCN (**I1**) in mechanism *A*, the rate-limiting step remains the HCN to HNC isomerization since the **TS1** 50 K free-energy barrier is equal
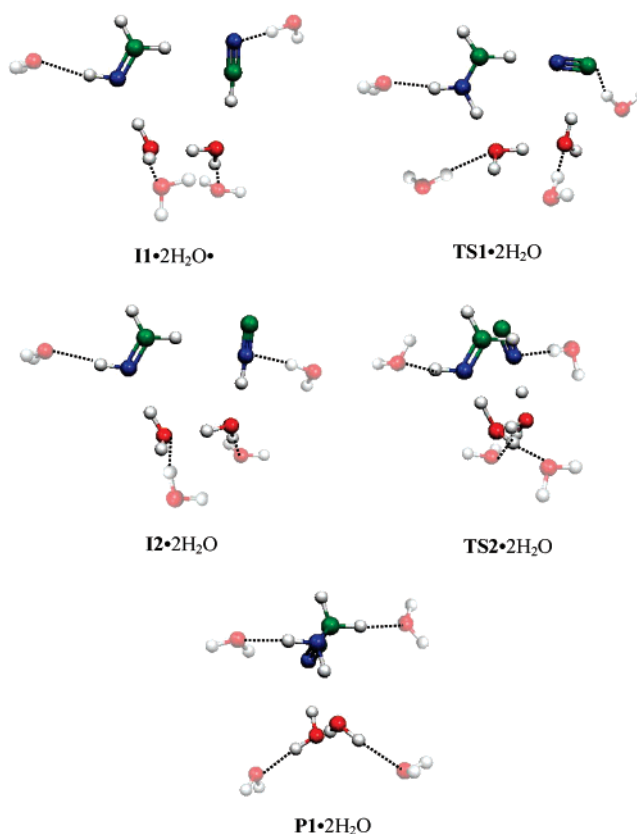

Figure 8. Optimized geometries at the B3LYP/6-311+G(d,p) level of theory for the reaction species involved in pathway *A* for the core reaction system + 12 H$_2$O as explicit external solvation. For clarity, only the external solvating waters that are directly hydrogen-bonded (dotted line) to the core reaction system are shown. The color scheme for the atoms is blue for N, green for C, red for O, and white for H. Interatomic distances are given in Å.

TABLE 3: Relative Thermodynamic Contributions for the Reaction Intermediates of the Core Reaction System with 2 H$_2$O in the Ring and 12 H$_2$O as External Solvent[a]

	I1	TS1	I2	TS2	TS4	P1	TS3	P2
ΔE	0	11.5	9.1	10.7	7.1	−14.7	6.9	3.6
$\Delta E^{\ddagger b}$		I1→TS1: 11.5		I2→TS2: 1.3	I1→TS4: 7.1		P2→TS3: 3.3	
$\Delta\Delta E^{\ddagger\ddagger c}$		−16.7		−10.6	−12.3		−15.1	
$\Delta G_{50K}{}^d$	0	10.9	9.2	9.9	6.3	−15.1	6.1	2.7
$\Delta G^{\ddagger}_{50K}{}^{d,e}$		I1→TS1: 10.9		I2→TS2: 0.7	I1→TS4: 6.3		P2→TS3: 3.4	
$\Delta\Delta G^{\ddagger}_{50K}{}^f$		−16.7		−10.5	−12.3		−14.8	

[a] Calculated with B3LYP/6-31+G(d,p) and including ZPE corrections. The corresponding **I1** complex is the reference. *[b]* ZPE-corrected energy barrier separating the indicated stable intermediate from the following adjacent transition state. *[c]* Lowering of the ZPE-corrected energy barriers when adding 12 external H$_2$O compared to the case with no external solvation. *[d]* The 50 K free energies relative to **I1**, and $\Delta G^{\ddagger}_{50K}$ are the transition-state free-energy barriers relative to the stable species indicated. *[e,f]* Same as footnotes *b* and *c*, respectively, for the 50 K relative free energy.

to 10.9 kcal/mol even when explicit solvation is included. Production of aminoacetonitrile from HCN in the ISM would be very difficult with such a barrier. Following now the direct mechanism *B* from the HCN complex **I1**, the 50 K free-energy barrier for the rate-limiting step (**TS4**) is smaller by almost 5.0 kcal/mol than the barrier calculated for the indirect mechanism *A* from the HCN complex **I1**. However, such a barrier for the reaction starting with HCN remains still significant in the low-temperature ISM.

Formation of the Aminoacetonitrile Precursor of Glycine

J. Phys. Chem. C, Vol. 112, No. 8, 2008 **2979**
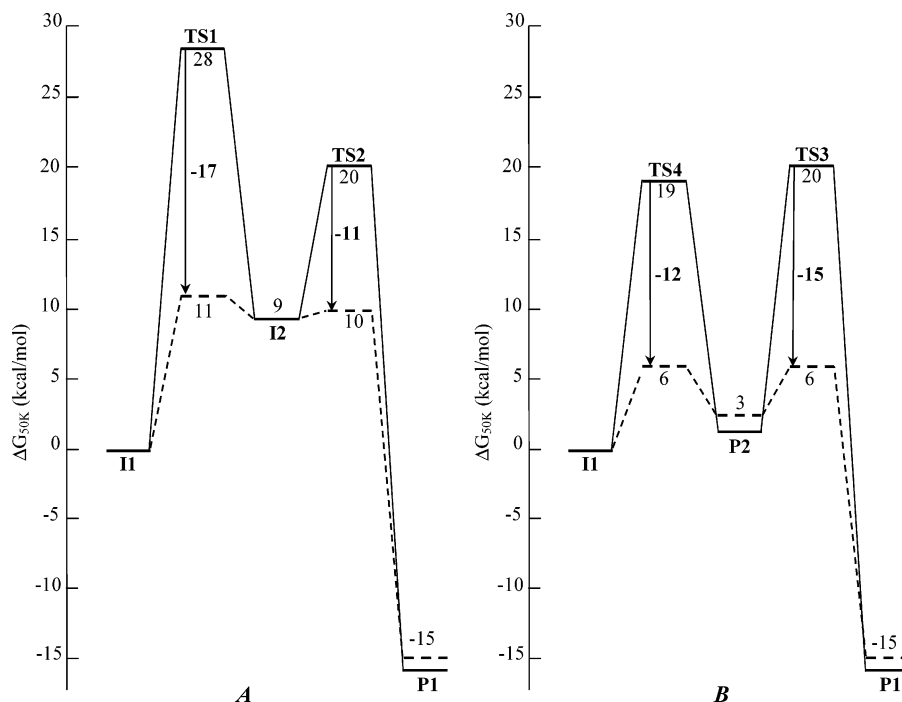
Figure 9. Relative free-energy profile (kcal/mol) computed at $T = 50$ K along reaction pathways *A* and *B* (see Figure 1) for the CRS alone (solid) and the CRS with 12 external solvating H_2O's (dashed). Note that the values of the free energies in Table 3 are rounded in this figure. For optimized structures of the intermediates, see Figures 5 and 8.

The central conclusion is that for the one-step mechanism with HNC as a reactant (pathway *A*), that is, starting with **I2**, the free-energy barrier is only 0.7 kcal/mol at 50 K, making aminoacetonitrile production via this route feasible in the ISM. In contrast, for the reaction for producing aminoacetonitrile starting with HCN, the barriers (∼11 kcal/mol via mechanism *A* and ∼6 kcal/mol via mechanism *B*) are substantially under the low-temperature conditions of the ISM. Finally, it is important to note that the low-barrier HNC reaction starting with **I2** in pathway *A* can avoid a "short-circuiting" return to the unproductive HCN isomer; the forward barrier of 0.7 kcal/mol to produce aminoacetonitrile is about half that of the reverse isomerization HNC → HCN.

VI. Concluding Remarks

The reaction between methanimine CH_2NH with HCN and HNC to produce aminoacetonitrile H_2NCH_2CN on a model interstellar icy grain surface has been investigated as a key penultimate step in the possible formation of the amino acid glycine in the interstellar medium (ISM) via a Strecker synthesis route.

The principal conclusion is that a proton relay mechanism involving two water molecules in a ring structure with the reactants, together with sufficient external solvation by further waters, allows the feasibility of the reaction between the HNC isomer and methanimine under ISM conditions, with an estimated free-energy barrier of 0.7 kcal/mol at 50 K. On the other hand, a barrier of ∼6 kcal/mol is estimated for the corresponding reaction with the HCN isomer in the most favorable mechanism.

Both HNC and HCN are present in the ISM in comparable amounts.[10] The present calculations on the modeled ice surface indicate that in the presence of methanimine, the isomerization of HNC to the effectively nonreactive isomer HCN has a 50 K free-energy barrier approximately twice that of the barrier for—and thus does not "short circuit"—the desired HNC reaction with methanimine. The HNC → HCN isomerization on an ice surface

when a HNC molecule is not a nearest neighbor of a methanimine molecule is examined elsewhere,[29] with the conclusion that this isomerization is feasible under ISM conditions. On the basis of the estimated 50 K isomerization rate, approximate estimates of the surface diffusion constant of HNC suggest that the reaction of HNC with methanimine probably requires that HNC and methanimine are, or are close to being, initially nearest neighbors.

The present conclusion of the feasibility of the penultimate step in the Strecker synthesis route to glycine on icy grain particles leaves open the viability of the final step of the hydrolysis of aminoacetonitrile to generate the amino acid. Takano et al. have suggested that amino acid precursors, such as aminoacetonitrile, are more stable toward photodestruction by UV radiation than their amino acid analogues.[30] As such, aminoacetonitrile could be formed in the ISM and then transported to earth in comets or meteorites where it undergoes hydrolysis. The reaction pathways and conditions necessary for the hydrolysis of aminoacetonitrile are presently under study.[31]

References and Notes

(1) (a) Charnley, S. B.; Rodgers, S. D.; Kuan, Y.-J.; Huang, H.-C. *Adv. Space Res.* **2002**, *30*, 1419. (b) Combes, F.; Rieu, N. Q.; Wlodarczak, G. *Astron. Astrophys.* **1996**, *308*, 618. (c) de Duve, C. *Origins Life Evol. Biospheres* **2003**, *33*, 559. (d) Ehrenfreund, P.; Bernstein, M. P.; Dworkin, J. P.; Sandford, S. A.; Allamandola, L. J. *Astrophys. J.* **2001**, *550*, L95. (e) Ehrenfreund, P.; Irvine, W. M.; Becker, L.; Blank, J.; Brucato, J. R.; Colangeli, L.; Derenne, S.; Despois, D.; Dutrey, A.; Fraaije, H.; Lazcano, A.; Owen, T.; Robert, F. *Rep. Prog. Phys.* **2002**, *65*, 1427. (f) Krewlowski, J. *Adv. Space Res.* **2002**, *30*, 1395. (g) Miller, S. L. *Science* **1953**, *117*, 528. (h) Miller, S. L. *J. Am. Chem. Soc.* **1955**, *77*, 2351. (i) Pohorille, A. *Adv. Space Res.* **2002**, *30*, 1509. (j) Rodgers, S. D.; Charnley, S. B. *Mon. Not. R. Astron. Soc.* **2001**, *320*, L61. (k) Schutte, W. A. *Adv. Space Res.* **2002**, *30*, 1409. (l) Shevlin, P. B.; McPherson, D. W.; Meliud, P. *J. Am. Chem. Soc.* **1983**, *105*, 488. (m) Tielens, A. G. G. M.; Charnley, S. B. *Origins Life Evol. Biospheres* **1997**, *27*, 23. (n) Winnewisser, G.; Herbst, E. *Rep. Prog. Phys.* **1993**, *56*, 1209.

(2) (a) Bernstein, M. P.; Dworkin, J. P.; Sandford, S. A.; Cooper, G. W.; Allamandola, L. J. *Nature* **2002**, *416*, 401. (b) Munoz Caro, G. M.; Meierhenrick, U. J.; Schutte, W. A.; Barbier, B.; Arcones, S. A.; Rosenbauer, H.; Thiemann, W. H.-P.; Brack, A.; Greenberg, J. M. *Nature* **2002**, *416*, 403.

(3) (a) Chyba, C.; Sagan, D. *Nature* **1992**, *335*, 125. (b) Ehrenfreund, P.; Glavin, D. P.; Botta, O.; Cooper, G.; Bada, J. L. *Proc. Natl. Acad. Sci. U.S.A.* **2001**, *98*, 2138. (c) Shock, E. L. *Nature* **2002**, *416*, 380.

(4) (a) Botta, G.; Glavin, D. P.; Kminek, G.; Bala, J. L. *Origins Life Evol. Biosphere* **2002**, *32*, 143. (b) Cronin, J. R.; Pizzarello, S. *Adv. Space Res.* **1983**, *3*, 1983. (c) Walch, S. P.; Bakes, E. L. O. *Chem. Phys. Lett.* **2001**, *346*, 267. (d) Woon, D. E. *Astrophys. J.* **2002**, *571*, L177.

(5) (a) Kuan, Y.-J.; Charnley, S. B.; Huang, H.-C.; Tseng, W. L.; Kisiel, Z. *Astrophys. J.* **2003**, *593*, 848. (b) Snyder, L. E.; Lovas, F. J.; Hollis, J. M.; Friedel, D. N.; Jewell, P. R.; Remijan, A.; Ilyushin, V. V.; Alekseev, E. A.; Dyubko, S. F. *Astrophys. J.* **2005**, *619*, 914.

(6) Ehrenfreund, P.; Fraser, H. *Solid State Astrochem.* **2003**, *120*, 317.

(7) (a) Bada, J. L.; Lazcano, A. *Nature* **2002**, *416*, 475. (b) Coxon, J. M.; Norman, R. O. C. *Principles of Organic Synthesis*, 3rd ed.; Kluwer Academic Publishers: Dordrecht, The Netherlands, 1993. (c) Duthaler, R. O. *Tetrahedron* **1994**, *50*, 1539. (d) Groger, H. *Chem. Rev.* **2003**, *103*, 2795. (e) Li, J.; Jiang, W.-Y.; Han, K.-L.; He, G.-Z.; Li, C. *J. Org. Chem.* **2003**, *68*, 8786. (f) Sorrell, T. N. *Organic Chemistry*; University Science Books: Herndon, VA, 1999. (g) Strecker, A. *Ann. Chem. Pharm.* **1850**, *75*, 27. (h) Williams, R. M.; Hendrix, J. A. *Chem. Rev.* **1992**, *92*, 889. (i) Yet, L. *Angew. Chem., Int. Ed.* **2001**, *40*, 875.

(8) (a) Allamandola, L. J.; Bernstein, M. P.; Sandford, S. A.; Walker, R. L. *Space Sci. Rev.* **1999**, *90*, 219. (b) d'Hendecourt, L.; Dartois, E. *Spectrochim. Acta, Part A* **2001**, *57*, 669. (c) Ehrenfreund, P.; Charnley, S. B. From Astrochemistry to Astrobiology; Proceedings of the First European Workshop on Exo/Astrobiology, Frascati, Italy, 2001; ESA-SP-496. (d) Ehrenfreund, P.; Dartois, E.; Demyk, K.; D'Hendecourt, L. *Astron. Astrophys.* **1998**, *339*, L17. (e) Ehrenfreund, P.; Fraser, H. J. *Solid State Astrochemistry*; Kluwer Academic Press: The Netherlands, 2002. (f) Van Dishoeck, E. F. *Faraday Discuss.* **1998**, *109*, 31. (g) Williams, D. A.; Herbst, E. *Surf. Sci.* **2002**, *500*, 823. (h) Woon, D. E. Ab Initio Quantum Chemical Studies of Reactions in Astrophysical Ices—Reactions Involving CH_3OH, CO_2, CO, and HNCO in $H_2CO/NH_3/H_2O$ Ices. In *Astrochemistry: From Laboratory Studies to Astronomical Observations*, AIP Conference Proceedings; Kaiser, R. I., Bernath, P., Mebel, A. M., Osamura, Y., Petrie, S., Eds.; Springer: New York, 2006; Vol. 855, p 305.

(9) Ehrenfreund, P.; Charnley, S. B. *Annu. Rev. Astron. Astrophys.* **2000**, *38*, 427.

(10) Arnaud, R.; Adamo, C.; Cossi, M.; Milet, A.; Vallee, Y.; Barone, V. *J. Am. Chem. Soc.* **2000**, *122*, 324.

(11) Smith, M. B. *Organic Synthesis*, 2nd ed.; McGraw-Hill Higher Education: New York, 2002.

(12) Greenberg, J. M. *Surf. Sci.* **2002**, *500*, 793.

(13) Basiuk, V. A. *J. Phys. Chem. A* **2001**, *105*, 4252.

(14) (a) Irvine, W. M.; Bergin, E. A.; Dickens, J. E.; Jewitt, D.; Lovell, A. J.; Matthews, H. E.; Schloerb, F. P.; Senay, M. *Nature* **1998**, *393*, 547. (b) Irvine, W. M.; Bockelee-Morvan, D.; Lis, D. C.; Matthews, H. E.; Biver, N.; Crovisier, J.; Davies, J. K.; Dent, W. R. F.; Gautier, D.; Godfrey, P. D.; Keene, J.; Lovell, A. J.; Owen, T. C.; Phillips, T. G.; Rauer, H.; Schloerb, F. P.; Senay, M.; Young, K. *Nature* **1996**, *383*, 418. (c) Irvine, W. M.; Schloerb, F. P. *Astrophys. J.* **1984**, *282*, d. (d) Schilke, P.; Walmsley, C. M.; Forets, G. P. d.; Roueff, E.; Flower, D. R.; Guilloteau, S. *Astron. Astrophys.* **1992**, *256*, 595.

(15) (a) Bianco, R.; Hynes, J. T. *J. Phys. Chem. A* **1998**, *102*, 309. (b) Bianco, R.; Hynes, J. T. *J. Phys. Chem. A* **1999**, *103*, 3797.

(16) Woon, D. E. *Icarus* **2001**, *149*, 277.

(17) Schmidt, M. W.; Baldridge, K. K.; Boatz, J. A.; Elbert, S. T.; Gordon, M. S.; Jensen, J. H.; Koseki, S.; Matsunaga, N.; Nguyen, K. A.; Su, S. J.; Windus, T. L.; Dupuis, M.; Montgomery, J. A. *J. Comput. Chem.* **1993**, *14*, 1347.

(18) (a) Becke, A. D. *J. Chem. Phys.* **1993**, *98*, 5648. (b) Lee, C.; Yang, W.; Parr, R. G. *Phys. Rev. B* **1988**, *37*, 785.

(19) Basiuk, V. A.; Escobar, A. H. C.; Molina, H. M. M. *Int. J. Quantum Chem.* **2002**, *87*, 101.

(20) (a) Binkley, J. S.; Pople, J. A. *Int. J. Quantum Chem.* **1975**, *9*, 229. (b) Hariharan, P. C.; Pople, J. A. *Chem. Phys. Lett.* **1972**, *66*, 217. (c) Krishnan, R.; Frisch, M. J.; Pople, J. A. *J. Chem. Phys.* **1980**, *72*, 4244.

(21) Andzelm, J.; Wimmer, E. *J. Chem. Phys.* **1992**, *96*, 1280.

(22) Jorgensen, P.; Jensen, H. J.; Helgaker, T. *Theor. Chim. Acta* **1988**, *73*, 55.

(23) Sun, J.; Ruedenberg, K. *J. Chem. Phys.* **1993**, *98*, 9707.

(24) For a large number of reactions, calculations performed with the B3LYP/6−31G** model chemistry yield activation energies in better agreement with experiment than higher-level model chemistries. This observation is attributed to error cancellation, on the one hand, the error due to the small basis set employed and, on the other hand, the difficulty of using the B3LYP functional to treat long-range interactions. See, for example, Hermida-Ramón, J. M.; Rodríguez-Otero, J.; Cabaleiro-Lago, E. M. *J. Phys. Chem. A* **2003**, *107*, 1651.

(25) (a) Barone, V.; Cossi, M. *J. Phys. Chem. A* **1998**, *102*, 1995. (b) Barone, V.; Cossi, M.; Tomasi, J. *J. Chem. Phys.* **1997**, *107*, 3210. (c) Cances, M. T.; Mennucci, V.; Tomasi, J. *J. Chem. Phys.* **1997**, *107*, 3032. (d) Cossi, M.; Barone, V.; Cammi, R.; Tomasi, J. *Chem. Phys. Lett.* **1996**, *255*, 327. (e) Miertus, S.; Scrocco, E.; Tomasi, J. *J. Chem. Phys.* **1981**, *55*, 117. (f) Miertus, S.; Tomasi, J. *J. Chem. Phys.* **1982**, *65*, 239.

(26) Mulliken, R. S. *J. Chem. Phys.* **1955**, *23*, 1833.

(27) Arnaud et al. (see ref 10) calculated the solvation free energy of the gas-phase reaction using a complex procedure. They adopted the more conventional set of Pauling radii for generating the solute cavities, which give less reliable absolute solvation energies. Their results reveal that absolute values of solvation energies do not naturally lead to a reliable evaluation of the relative values. In their calculation of HCN + CH_2NH with two explicit H_2O molecules, $\Delta G + \Delta G$(PCM) values are more than 10 kcal/mol for several transition states, whereas our calculations using the standard PCM model within the GAMESS program give lower free-energy barriers (7.2 kcal/mol for **TS4**, for example).

(28) (a) Xu, S.; Zhao, X. S. *Acta Phys. Chem. Sin.* **1998**, *14*, 988. (b) Xu, S.; Zhao, X. S. *Acta Phys. Chem. Sin.* **1999**, *15*, 193. (c) Xu, S. C. *J. Chem. Phys.* **1999**, *111*, 2242. (d) Xu, S. C.; Zhao, X. S. *J. Phys. Chem. A* **1999**, *103*, 2100.

(29) Koch, D. M.; Toubin, C.; Xu, S.; Peslherbe, G. H.; Hynes, J. T. *J. Phys. Chem. C* **2007**, *111*, 15026.

(30) Takano, Y.; Ohashi, A.; Kaneko, T.; Kobayashi, K. *App. Phys. Lett.* **2004**, *84*, 1410.

(31) Some aspects of the hydrolysis step have been considered in Zhu, H.-S.; Ho, J.-J. *J. Phys. Chem. A* **2004**, *108*, 3798, although with minimal solvation and without exploration of the possibility of acid or base catalysis of the hydrolysis (see, for example, Smith, M. B.; March, J. *March's Advanced Organic Chemistry: Reactions, Mechanisms, and Structure*, 5th ed.; John Wiley: New York, 2001.)

(32) In this connection, we note the existence of the article Xu, S.; Wang, N. *Acta Phys.-Chim. Sin.*, **2007**, *23*, 212−216.